Reliability and Energy Loss in Full-scale Wind Power Converter Considering Grid Codes and Wind Classes

Zhou, Dao; Blaabjerg, Frede; Franke, Toke; Tonnes, Michael; Lau, Mogens

Published in:
Proceedings of the 2014 IEEE Energy Conversion Congress and Exposition (ECCE)

DOI (link to publication from Publisher):
10.1109/ECCE.2014.6953817

Publication date:
2014

Reliability and Energy Loss in Full-scale Wind Power Converter Considering Grid Codes and Wind Classes

Dao Zhou, Frede Blaabjerg
Department of Energy Technology
Aalborg University
Aalborg, Denmark
zda@et.aau.dk; fbl@et.aau.dk

Toke Franke, Michael Tonnes
Danfoss Silicon Power GmbH
Flensburg, Germany
toke.franke@danfoss.com; michael.tonnes@danfoss.com

Mogens Lau
Siemens Wind Power A/S
Brande, Denmark
mogens.lau@siemens.com

***Abstract*—With the increasing penetration of the wind power, reliable operation and cost-effective wind energy production are of more and more importance. As one of the promising configurations, the cost on reliability and production losses of permanent-magnet synchronous generator based full-scale wind power converter is studied considering the grid code with reactive power production as well as the annual wind profile. Regarding the reliability, it is found that either the Over-Excited (OE) or the Under-Excited (UE) reactive power injection threatens the lifespan under all wind classes. Meanwhile, if the specific designed wind turbine system operates at different wind classes, it can be seen that higher wind class level results in lower lifetime of the power converter. In respect to the cost of the reactive power, either the OE or the UE reactive power increases the energy loss per year significantly if they are provided all year around, in which the OE reactive power injection even has a worse scenario. Moreover, it is also concluded that in order to realize an energy loss saving of the wind turbine system, the constant power factor control strategy is more preferred compared to an extreme reactive power injection.**

I. INTRODUCTION

With the increasing penetration of wind power during recent decades, reliable operation and cost-effective wind energy production are of more and more importance [1]-[3]. Due to the fact that the wind turbine system is required to behave like a conventional synchronous generator (including the capability of the active power and the reactive power) and to overcome the Low Voltage Ride-Through (LVRT), the Permanent-Magnet Synchronous Generator (PMSG) based configuration might become attractive seen from the wind turbine manufacturers [4], since the employed power electronic converter can handle the full-scale of generator power and decouple the grid and the generator.

Another tendency of the wind power development is the popularity of the offshore wind farms, which pushes the wind turbine system to operate with reliable and cost-effective performance. Reliability and robustness of the system are closely related to its mission profile - the representation of all relevant conditions that the system will be exposed to in all of its intended application throughout its entire life cycle [5]. Then the failure may happen during the violation of the strength and stress analysis, in which the stressor factors may be due to the environmental loads (like thermal, mechanical, humidity, etc.), or the functional loads (such as usage profiles, electrical operation). Among the stressors distribution, the thermal cycling accounts for more than a half of the failure probability [5]. On the basis of the universal approach of power semiconductor device reliability assessment stated in [6]-[8], the lifespan of the vulnerable power electronic converter is focused on in terms of thermal cycling caused by the alternative current with one fundamental period.

Widely use of the renewable energy tightly relies on the Levelized Cost Of Electricity (LCOE), whose value is expected to be lower than the traditional fossil energy by the end of the 2030 according to a German report [9]. As studied in [10], [11], the higher lifespan of the renewable energy plant or the higher annual energy production makes the LCOE decrease. Moreover, the produced energy per year of a typical PV plant is not only connected to the site environment (e.g. solar irradiance and ambient temperature), but also limited by the power conversion technology and the commands from the Transmission System Operator (TSO). Consequently, for wind power application, it is necessary to evaluate and analyze the effects of reactive power injection on the energy loss, which will be focused on in this paper.

The structure of this paper is organized as follows. A typical 2 MW PMSG system and the analytical approach to

978-1-4799-5776-7/14/$31.00 ©2014 IEEE

predict the power loss of power switching device are addressed in Section II. Then Section III focuses on the lifetime estimation of the power device seen from the thermal cycling point of view with various reactive power injections and various wind classes. Section IV discusses the annual energy production according to annual wind profile, and addresses the cost of energy loss regarding the various operational modes to inject reactive power. Finally, concluding remarks are drawn in Section V.

II. Loss Calculation of Power Device

A. Configuration of PMSG System

As the TSO recently tightens the LVRT capability of renewable energy system, a PMSG based wind turbine system with full-scale power converter is more widely employed due to its advantage of full power controllability [12]. The back-to-back power converter consists of the generator-side converter and the grid-side converter as shown in Fig. 1. For the generator-side converter, it keeps the rotor speed of the PMSG operating at the Maximum Power Point Traction (MPPT) and the transfers the active power from the wind to the grid. For the grid-side converter, it is designed not only for constant dc-link voltage, but also to provide the full amount of the reactive power required by the TSO. As only the grid-side converter is responsible to react to the grid code requirements, this part is mainly focused in this paper. A popular low-voltage 2 MW PMSG system is selected for a case study, and the parameters of the system are listed in TABLE I [13].

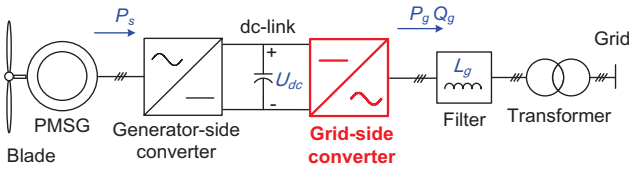

Fig. 1. Configuration of the full-scale power converter based permanent-magnet synchronous generator wind turbine system.

TABLE I

Basic Parameters of 2 MW PMSG System

Rated power P_g	2 MW
Rated line voltage amplitude U_{gm}	563 V
Rated loading current amplitude I_{gm}	2368 A
DC-link voltage U_{dc}	1.1 kV
Grid filter inductance L_g	0.15 mH (0.2 pu)
Line frequency f_1	50 Hz
Switching frequency f_s	2 kHz
Power modules inside grid-side converter leg	1 kA/1.7 kV; four parallel
Cut-in wind speed	4 m/s
Rated wind speed	12 m/s
Cut-out wind speed	25 m/s

B. Derterming Factors of Power Device Loading

If a simple inductor L_g is introduced as the grid filter shown in Fig. 2(a), Fig. 2(b) indicates that the amplitude of the converter output voltage u_c and output current i_g and displacement angle between them φ_{iu} can be expressed in terms of the active power P_g and reactive power Q_g [14],

$$i_g = \sqrt{\left(\frac{P_g}{1.5U_{gm}}\right)^2 + \left(\frac{Q_g}{-1.5U_{gm}}\right)^2} \tag{1}$$

$$u_c = \sqrt{\left(U_{gm} - \frac{X_g \cdot Q_g}{1.5U_{gm}}\right)^2 + \left(-\frac{X_g \cdot P_g}{1.5U_{gm}}\right)^2} \tag{2}$$

$$\varphi_{iu} = a\tan\left(\frac{Q_g}{P_g}\right) - a\tan\left(\frac{X_g \cdot P_g / 1.5U_{gm}}{U_{gm} - X_g \cdot Q_g / 1.5U_{gm}}\right) \tag{3}$$

where X_g denotes the grid filter reactance at the line frequency f_1. It is noted that for the grid-tied converter, the current stress of the power device is determined by the produced active power and reactive power as illustrated in (1), while the voltage stress of the power device, as stated in (2), is not only related to the above mentioned active and reactive power, but also linked to the value of the grid filter inductor.

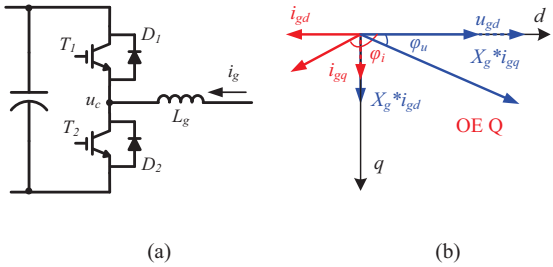

Fig. 2. Illustration of the grid-side converter. (a) One leg of the three-phase grid-tied converter; (b) Converter output current and voltage in d-q axis.

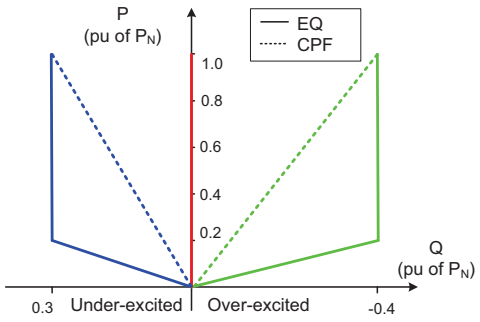

Fig. 3. Supportive reactive power range of modern wind power system stated in German grid codes [15].
Note: EQ denotes operation mode of the extreme reactive power injection and CPF denotes operation mode of the constant power factor.

It is well-known that reactive power is preferred for LVRT in order to rebuild the normal grid voltage for modern renewable energy system. Nevertheless, many pioneering countries of wind energy production (like Germany,

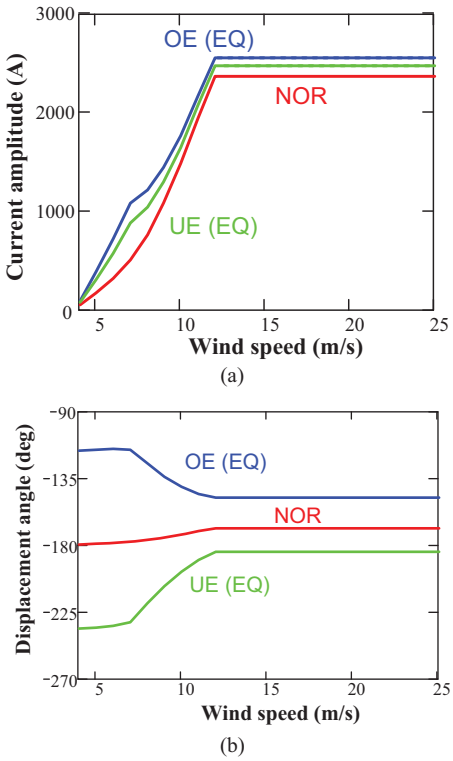

Fig. 4. Reactive power effects on power device loading. (a) Current amplitude versus wind speed; (b) Displacement angle versus wind speed.

Denmark, UK, etc.) have issued grid codes that during normal operation, the reactive power capacity is also defined. As shown in Fig. 3, one of the strictest grid requirements is established by German TSO, in which up to 40% Over-Excited (OE) and 30% Under-Excited (UE) reactive power is delivered if the produced active power is above 20%. Due to different control objectives – various amounts of reactive power injection for either the Extreme Reactive Power (EQ) or the Constant Power Factor (CPF) can be implemented. In the case of the CPF operation, the power factor of the OE reactive power injection is slightly smaller than the UE reactive power injection. Moreover, the whole supportive range of the reactive power is enveloped by the EQ operation.

According to a 2 MW wind turbine power curve [16], together with the reactive power requirement shown in Fig. 3, the envelope of the grid converter current amplitude and the displacement angle is calculated and shown in Fig. 4(a) and Fig. 4(b) from the cut-in 4 m/s until the cut-out 25 m/s, in which the maximum range of the reactive power as well as the no reactive power exchange (NOR) are taken into account. It is noted either the current amplitude or the displacement angle become constant if the wind speed reaches the rated 12 m/s. Moreover, the introduction of either the OE or the UE reactive power imposes additional current stress, which is consistent with (1). Another turning point occurs in the case of the reactive power compensation during the increase of the wind speed because the produced active power gets 0.2 pu at such wind speed. In respect to the displacement angle, the dominant reactive current at lower wind speed forces the converter current almost leading or lagging 90 degree compared to the converter voltage. However, at the higher wind speed, the converter current and voltage are nearly in opposite phase as the component of active current takes up the majority of the total current.

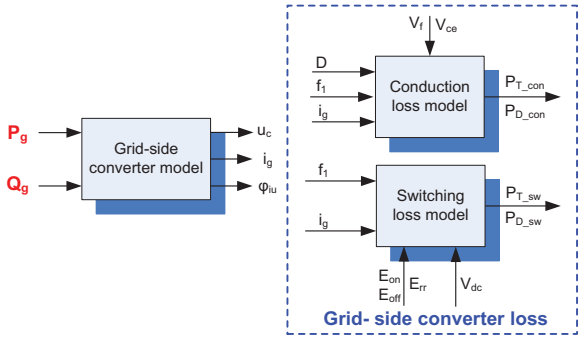

Fig. 5. Framework of power semiconductor loss evaluation in terms of the conduction loss and the switching loss.

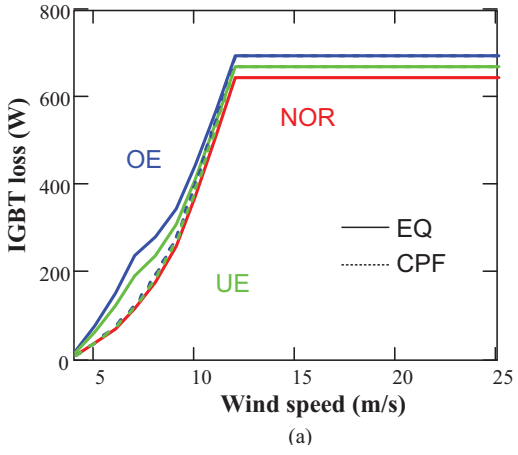

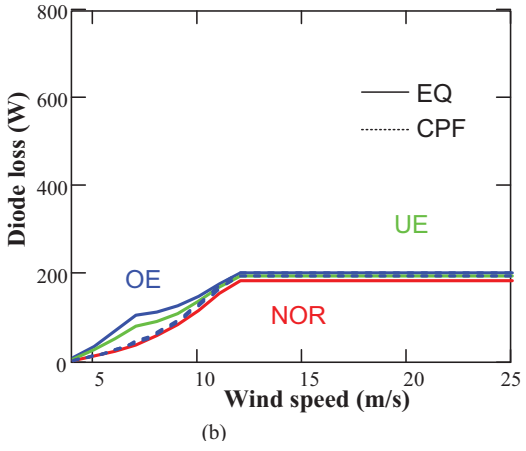

Fig. 6. Loss profile of power semiconductor. (a) IGBT loss; (b) Diode loss.

C. Calculation of Conduction Loss and Switching Loss

Because the change of reactive power alters the current loading of the power device, it is worth to translate this information further into the power dissipation of the power device. In fact, the loss dissipation of the power semiconductor has been studied a lot [17]-[19]. One of them is the physical model of power device during dynamic operation to see the different parasitic parameters influence [18]. Another popular approach, which mainly depends on the test data from power device manufacturer, the loss information during each switching pattern and conduction period could be calculated according to the datasheet, and the power loss is then accumulated by every switching pattern within the whole fundamental period of the loading current [19].

As shown in Fig. 5, the loss evaluation in this paper is based on the second approach – according the grid-side converter model as well as the conduction loss model and the switching loss model of the power device. Using conventional symmetrical space vector modulation [17], the power dissipation of the IGBT and the freewheeling diode can then analytically be calculated as shown in Fig. 6(a) and Fig. 6(b), respectively. It can be seen that the loading of the IGBT is heavier than the diode due to the direction of the active power flow. Furthermore, the loss in the case of the EQ and the CPF reactive power injection are both taken into account.

III. Operational Modes and Wind Classes Effects on Reliability

As the cost on maintenance in offshore wind farm is high, it pushes to the much higher lifespan of the entire wind turbine system. This section will address the impacts of the reactive power on power device reliability with various wind profiles and different operation modes.

A. Methods for Reliability Analysis

Thermal cycling of the junction temperature is caused by the cycling of power losses and it causes mechanical stress between joined materials with different expansion coefficients [6], [8]. Based on the previously mentioned loss evaluation method, the universal procedure of lifetime estimation is shown in Fig. 7. The mean junction temperature T_{jm} and the junction temperature variation of the most stressed dT_j of the power semiconductor can be obtained with the aid of Foster structure thermal model [7] as well as the total IGBT loss P_T and diode loss P_D. Then, together with the on-state time of the loading current within one cycle frequency t_{on}, which is the half value of the fundamental period [20], the power cycles can be calculated according to e.g. Coffin-Manson lifetime model [7]. Afterwards, the concept of the Consumed Lifetime (*CL*) is introduced,

$$\mathrm{CL_i} = \mathrm{D_i} \cdot \frac{365 \cdot 24 \cdot 3600 \cdot \mathrm{f_1}}{\mathrm{N_i}} \tag{4}$$

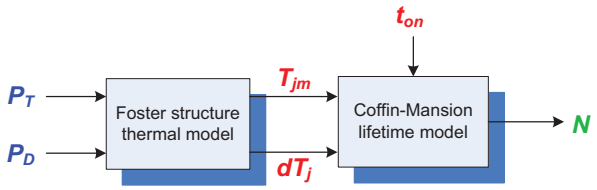

Fig. 7. Framework to estimate the power cycles of power semiconductor.

where subscript *i* denotes a certain wind speed from cut-in to cut-out, *D* denotes the wind speed probability of yearly wind speed, and *N* denotes the power cycles calculated by Fig. 7. CL_i denotes the power cycles consumed per year for the wind speed *i*.

Assuming that the damage accumulates linearly, the Miner's rule [7], [8] is applied in order to calculate the Total Consumed Lifetime (TCL),

$$\mathrm{TCL} = \sum_{\mathrm{i=4}}^{25} \mathrm{CL_i} \tag{5}$$

Due to the fact that the active power is fed into the grid through the grid-side converter, the IGBT is more stressed compared to the freewheeling diode as shown in Fig. 6. Consequently, for this specific power module, the reliability assessment of the grid-side converter only concerns about the IGBT chips.

B. Various Wind Classes

There are two common used density distributions of the wind speed – Weibull function and Rayleigh function. This paper applies for the Weibull distribution [21], which is characterized by a shape parameter of 2. As shown in Fig. 8, three scale parameters are used to represent various IEC wind class I, II and III [22], whose average wind speeds are 10 m/s, 8.5 m/s and 7.5 m/s, respectively. With the cut-in, rated and cut-out wind speed listed in TABLE I, four regions of wind distribution can be categorized.

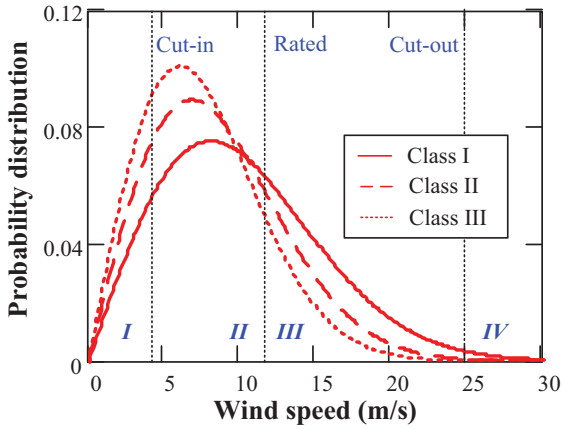

Fig. 8. Annual wind distribution with different wind classes defined by IEC standard [22].

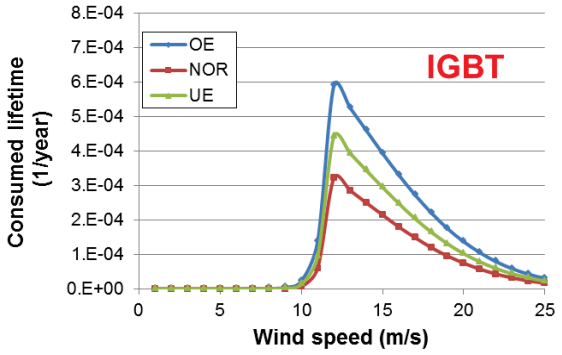

(a)

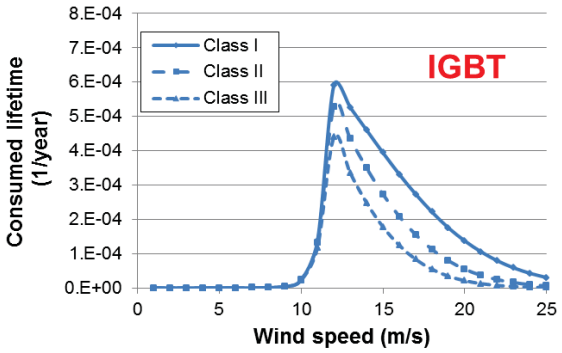

(b)

Fig. 9. Consumed lifetime of the IGBT at different wind speeds. (a) Various types of reactive power injection at Class I wind profile; (b) Various annual wind profile in the case of over-excited reactive power injection.

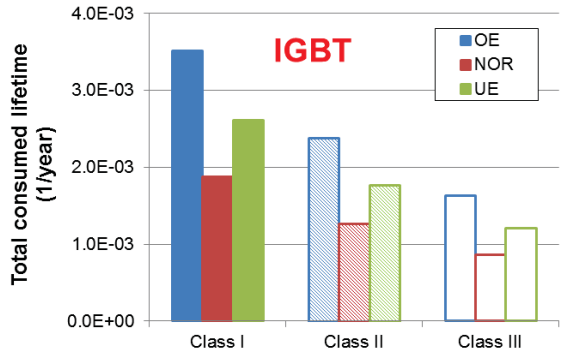

Fig. 10. Total consumed lifetime of the IGBT with various reactive types and various wind classes.

Applying the Class I wind profile as a case study, the consumed lifetime of the IGBT in various types of reactive power injections is shown in Fig. 9(a). It is evident that either the OE or the UE reactive power injection has higher CL compared to the NOR operation. Moreover, it can be seen that, as each wind speed above rated value has the same power cycles, the CL becomes changing consistent with the varying wind speed distribution shown in region III of Fig. 8. Furthermore, it is noted that the wind speed region below cut-in (region I in Fig. 8) and above cut-off wind speed (region IV in Fig. 8) have no contribution to the lifetime consumption.

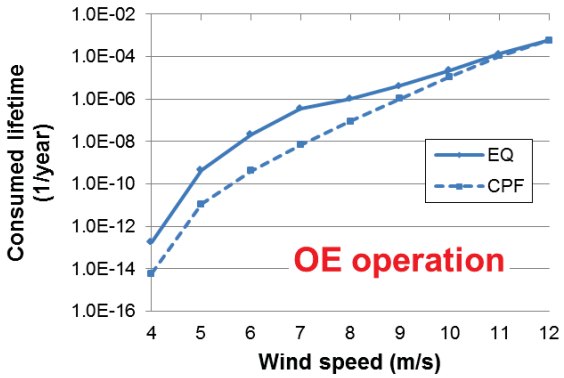

(a)

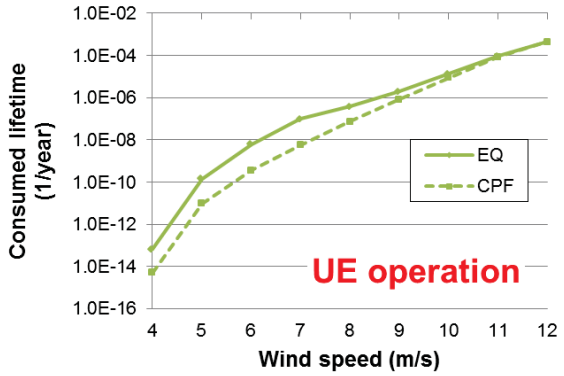

(b)

Fig. 11. Lifetime estimation with different operation modes according to Class I wind profile. (a) Over-excited reactive power injection; (b) Under-excited reactive power injection.

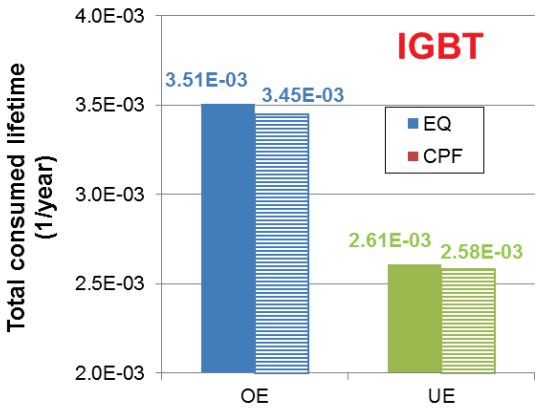

Fig. 12. Total consumed lifetime comparison with different operation modes.

As the OE reactive power has the most severe stress, this situation is used to further compare the effects of different wind profiles on the CL as shown in Fig. 9(b). Since the class I has the highest probability for region III wind speed, the CL of the class I wind profile is highest from the rated speed until the cut-out speed, followed by class II and class III wind profile.

As summarized in Fig. 10, for various types of reactive power injection, regardless of the class level of the wind profile, the OE reactive power injection reduces the lifetime most. In respect to various wind classes, it is noted that the higher class the wind level is, the lower lifetime of the power converter could be.

C. Operation modes of Reactive Power Injection

The effects of various operation modes on the lifetime consumption will be investigated. As shown in Fig. 3, the difference between the EQ and the CPF mainly lies in the wind speed region II from the cut-in to rated wind speed. Using Class I wind profile as a case study, a slight difference of the CL can be found both in the OE operation and the UE operation, as shown in Fig. 11(a) and Fig. 11(b). Consequently, a very small difference appears in the TCL shown in Fig. 12.

IV. Operatinal Modes and Wind Classes Effects on Energy Loss

With the increasing wind power proportion of the total energy production, the cost-effective operation to achieve the lower cost per kWh is preferred. This section is going to analyze the impacts of reactive power on the cost of energy.

A. Important concepts

As the entire loss of the grid-side converter is affected by various amounts of reactive power (either the types of the reactive power or the operation modes), together with the yearly wind speed distribution, the Energy Loss Per Year (ELPY – unit: MWh) can be predicted,

$$\mathrm{ELPY} = \sum_{i=4}^{12} \mathrm{P}_{\mathrm{GSC(n)}} \cdot \mathrm{T}_{\mathrm{(n)}} \tag{6}$$

where the P_{GSC} denotes the total power loss of the grid-side converter, including the total loss of IGBT switch and diode. T denotes the wind speed distribution as shown in Fig. 8. Subscript n denotes the wind speed. It is worth to mention that the ELPY is only of interest from the cut-in to the rated wind speed, because if the wind speed is higher than the rated value, it is assumed that the power loss dissipated in the PMSG system can be compensated from the mechanical power from the wind turbine blades.

The Annual Energy Production (AEP) from wind energy can also be obtained with the aid of the produced power P_g and the annual wind speed distribution T.

$$\mathrm{AEP} = \sum_{i=4}^{25} \mathrm{P}_{\mathrm{g(n)}} \cdot \mathrm{T}_{\mathrm{(n)}} \tag{7}$$

In respect to the AEP, the concerned wind speed is from the cut-in to cut-out wind speed.

The Annual Loss Of Energy (ALOE – unit: %) is achieved by dividing the ELPY from the AEP.

$$\mathrm{ALOE} = \frac{\mathrm{ELPY}}{\mathrm{AEP}} \cdot 100\% \tag{8}$$

As a result, Fig. 13 graphically shows the framework to predict the cost of energy loss in terms of the ELPY, AEP and ALOE.

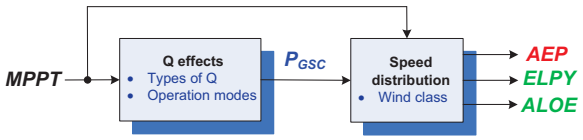

Fig. 13. Framework to predict the cost of energy loss in respect to the reactive power requirement from grid codes.

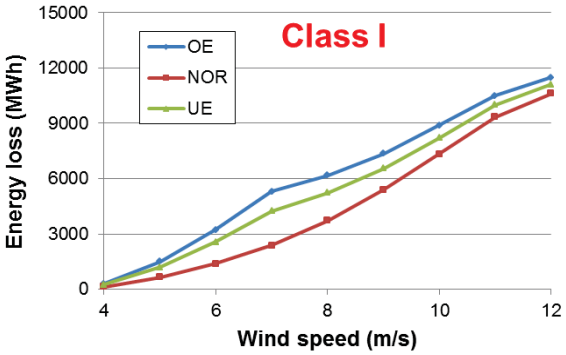

(a)

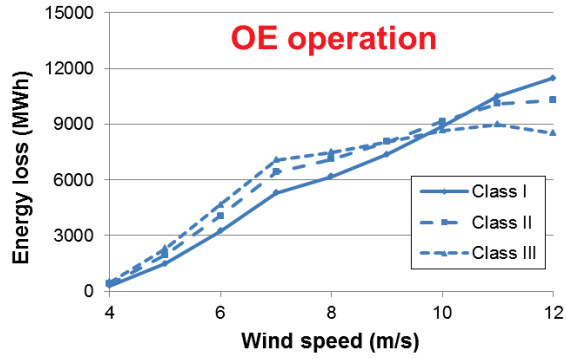

(b)

Fig. 14. Energy loss from cut-in to rated wind speed. (a) Various types of reactive power at Class I wind profile; (b) Various wind classes in case of OE reactive power.

B. Various Wind Classes

Taking Class I wind profile for example, the energy loss of the grid-side converter is shown in Fig. 14(a) at various types of reactive power injection. It is noted that only the

difference between the cut-in and rated wind speed is taken into account. Due to the fact that the OE reactive power imposes the energy loss most, this kind of the reactive power injection is then considered at various wind profiles. As shown in Fig. 14(b), it can be seen that the shape of the energy loss at each wind speed is consistent with the wind distribution in Fig. 8 at this specific strategy of the reactive power injection.

By adding the energy loss of the individual wind speed together, the ELPY is shown Fig. 15(a), in which either the UE or the OE reactive power injection increases the ELPY at all kinds of the wind classes. Moreover, regardless of reactive power type, it is interesting to see that all kinds of wind classes have almost similar EPLY. Due to the calculated AEP for each wind class, the ALOE is shown in Fig. 15(b). It is evident that the higher wind class is, the lower ALOE will be, because a higher wind class actually yields larger amount of the AEP. Besides, the highest ALOE 0.89 % appears at Class III, if the OE reactive power is injected all year around.

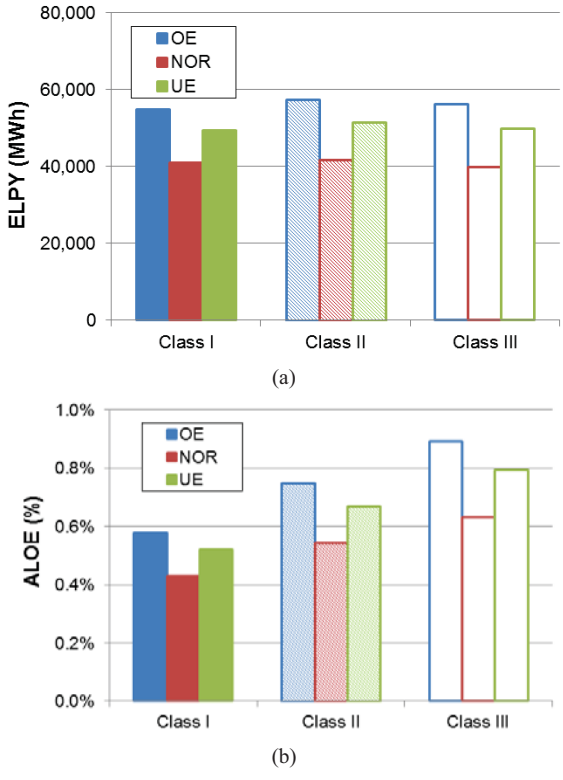

Fig. 15. Cost of energy with different wind classes. (a) Energy Loss Per Year (ELPY); (b) Annual Loss Of Energy (ALOE).

C. *Operation modes of Reactive Power Injection*

In respect to the operation modes at wind Class I, the EQ and the CPF reactive power injection is accordingly compared. As shown in Fig. 16, regardless the OE or UE reactive power, the CPF operation mode is more cost-effective than the EQ operation mode, as the consumed energy is less in the CPF mode.

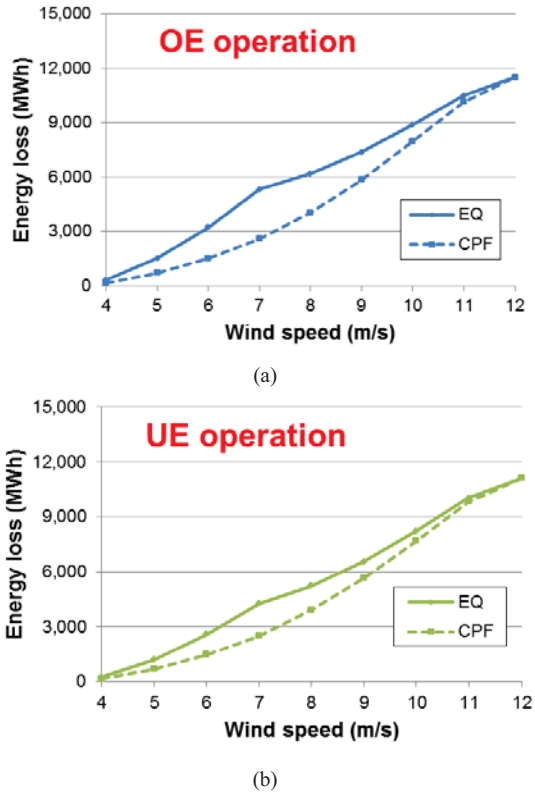

Fig. 16. Influence of the different operational modes on energy loss for a 2 MW wind turbine. (a) Over-excited reactive power injection; (b) Under-excited reactive power injection.

Consequently, as shown in Fig. 17(a), the CPF control scheme saves considerable energy either in the OE reactive power or the UE reactive power injection. According to Fig. 17(b), the ALOE reduce from 0.58% to 0.47% if the operation mode switches from the EQ to the CPF operation, implying 19.0% energy saving for the CPF compared to the EQ if the OE reactive power is required all year around. It is also applied to the UE reactive power injection, 13.5% energy saving can be obtained, if the control scheme changes from the EQ operation to the CPF operation.

V. CONCLUSION

This paper addresses a universal method to evaluate the loss dissipation inside the power switching device of wind power converter taking into account a number of operational modes. It is clear that the loss breakdown of the power device is jointly dependent on the active power reference from the MPPT algorithm and the required reactive power reference from the TSO. If the reactive power is injected according to the German grid codes, the cost on reliability and loss production are then evaluated in terms of various wind classes and operation modes.

In respect to reliability, it can be seen that either the OE or the UE reactive power significantly reduces the lifetime - the OE reactive power has the worst scenario. If different mission profiles are taken into consideration, it is concluded that higher wind class level has shorter lifespan of the power converter. Meanwhile, it is evident that a small difference of the total consumed lifetime occurs with various operational modes – the extreme reactive power and the constant power factor control strategies.

Regarding the energy loss, the introduction of the reactive power, either the OE reactive power or the UE reactive power, considerably imposes the energy loss per year, in which the OE reactive power has the worst scenario. However, when the different wind profiles are taken into account, similar energy loss per year is unexpectedly observed. Moreover, it is found that the constant power factor control scheme is preferred due to its energy saving at 19.0% and 13.5%, if the OE and the UE reactive power are provided all year around.

REFERENCES

[1] F. Blaabjerg, K. Ma, "Future on power electronics for wind turbine systems," *IEEE Journal of Emerging and Selected Topics in Power Electronics*, vol. 1, no. 3, pp. 139-152, Sept. 2013.

[2] H. Polinder, J. A. Ferreira, B. B. Jensen, A. B. Abrahamsen, K. Atallah, R. A. McMahon, "Trends in wind turbine generator systems," *IEEE Journal of Emerging and Selected Topics in Power Electronics*, vol. 1, no. 3, pp. 174-185, Sept. 2013.

[3] H. Wang, M. Liserre, F. Blaabjerg, P. Rimmen, J. Jacobsen, T. Kvisgaard, J. Landkildehus, "Transitioning to physics-of-failure as a reliability driver in power electronics," *IEEE Journal of Emerging and Selected Topics in Power Electronics*, vol. 2, no. 1, pp. 97-114, Mar. 2014.

[4] M. Liserre, R. Cardenas, M. Molinas, J. Rodriguez, "Overview of multi-MW wind turbines and wind parks," *IEEE Trans. Industrial Electronics*, vol. 58, no. 4, pp. 1081-1095, Apr. 2011.

[5] "ZVEI - Handbook for robustness validation of automotive electrical/electronic modules," Jun. 2013.

[6] ABB Application Note, Load-cycling capability of HiPaks, 2004.

[7] K. Ma, M. Liserre, F. Blaabjerg, T. Kerekes, "Thermal loading and lifetime estimation for power device considering mission profiles in wind power converter," *IEEE Trans. on Power Electronics*, IEEE Early Access.

[8] L. Wei, R. J. Kerkman, R .A. Lukaszewski, H. Lu, Z. Yuan, "Analysis of IGBT power cycling capabilities used in doubly fed induction generator wind power system," *IEEE Trans. on Industry Applications*, vol. 47, no. 4, pp. 1794-1801, Jul. 2011.

[9] C. Kost, J. Mayer, J. Thomsen, Levelized cost of electricity renewable energy technologies. (website: www.ise.fraunhofer.de)

[10] E. Koutroulis, F. Blaabjerg, "Design optimization of transformerless grid-connected PV inverters including reliability," *IEEE Trans. on Power Electronics*, vol. 28, no. 1, pp. 325-335, Jan. 2013.

[11] X. Yu, A. M. Khambadkone, "Reliability analysis and cost optimization of parallel-inverter system," *IEEE Trans. on Industrial Electronics*, vol. 59, no. 10, pp. 3881-3889, Oct. 2012.

[12] J. Dai, D. Xu, B. Wu, "A novel control scheme for current-source-converter-based PMSG wind energy conversion systems," *IEEE Trans .on Power Electronics*, vol. 24, no. 4, pp. 963-972, Apr. 2009.

[13] D. Zhou, F. Blaabjerg, M. Lau, M. Tonnes, "Thermal analysis of multi-MW two-level wind power converter," *in Proc. of IECON 2012*, pp. 5862-5868, 2012.

[14] D. Zhou, F. Blaabjerg, M. Lau, M. Tonnes, "Thermal behavior optimization in multi-MW wind power converter by reactive power circulation," *IEEE Trans. on Industry Applications*, vol. 50, no. 1, pp. 433-440, Jan. 2014.

[15] E.ON-Netz. Requirements for offshore grid connections, Apr. 2008.

[16] Vestas, V-90 wind turbine. (Website: http://www.vestas.com).

[17] J. W. Kolar, H. Ertl, Franz C. Zach, "Influence of the modulation method on the conduction and switching losses of a PWM converter system," *IEEE Trans. on Industry Applications*, vol. 27, no. 6, pp. 1063-1075, Nov. 1991.

[18] Y. Ren, M. Xu, J. Zhou, F. C. Lee, "Analytical loss model of power MOSFET," *IEEE Trans. on Power Electronics*, vol. 21, no. 2, pp. 310-319, Mar. 2006.

[19] B. Backlund, R. Schnell, U. Schlapbach, R. Fischer, E. Tsyplakov, "Applying IGBTs", ABB Application Note, Apr. 2009.

[20] D. Zhou, F. Blaabjerg, M. Lau, M. Tonnes, "Thermal profile analysis of doubly-fed induction generator based wind power converter with air and liquid cooling methods," *in Proc. of EPE 2013*, pp. 1-10, 2013.

[21] The Swiss wind power data website. (Website: http://wind-data.ch/tools/weibull.php)

[22] Wind turbines – part I: design requirements", IEC 61400-1, 3rd edition.

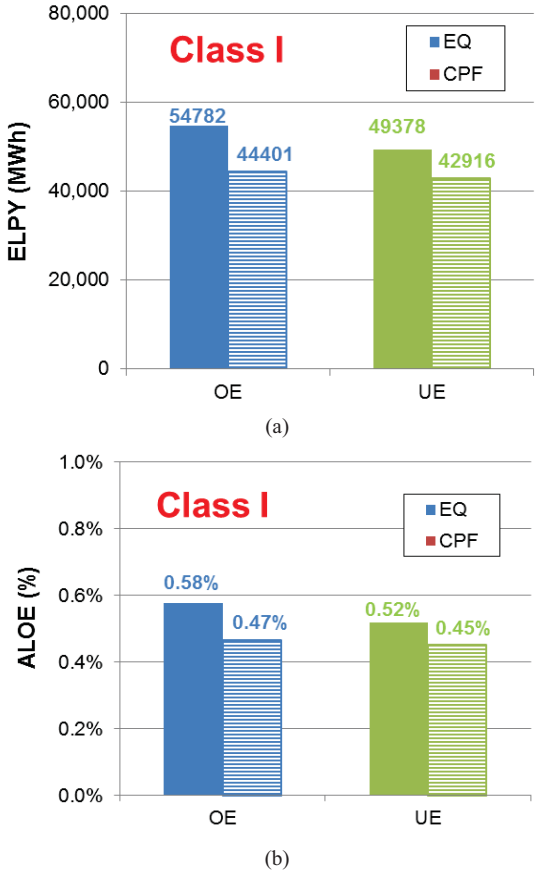

Fig. 17. Energy loss per year with different operation mode under wind Class I. (a) Energy Loss Per Year (ELPY); (b) Annual Loss Of Energy (ALOE).